

Article

Statistical Analysis of Heavy Rains and Floods around the French Mediterranean Basin over One Half a Century of Observations

Zeineddine Nouaceur¹, Ovidiu Murarescu^{2,*} and George Muratoreanu^{2,*}¹ UMR IDÉES CNRS 6266, Rouen University, Mont-Saint-Aignan CEDEX, 76821 Rouen, France² Department of Geography, Valahia University, 130001 Târgoviște, Romania

* Correspondence: ovidiu.murarescu@valahia.ro (O.M.); george.muratoreanu@valahia.ro (G.M.); Tel.: +40-726689917 (O.M.); +40-722291769 (G.M.)

Abstract: The French region adjacent to the Mediterranean basin is vulnerable to hydrological risks generated by convective precipitation in the form of heavy rainfall and conditioned by the configuration of the relief. These risks are driven by the increase in sea water temperature over the last half century, which itself has been more pronounced since 1990. The statistical analysis on the frequency of rainfall intensity in a 24 to 48 h interval, correlated with the NAO, WMOI and SSTMED indices shows a recrudescence of rainfall amounting to more than 100 mm, which leads to the genesis of floods and flash floods. Furthermore, there has been a higher frequency of floods and disasters in this period. The intensity of material and human damage recorded following such local Cévennes-type phenomena is also due to urban development and population growth.

Keywords: Mediterranean episode; Cevennes episode; heavy rainfall; flooding; the Mediterranean Sea



Citation: Nouaceur, Z.; Murarescu, O.; Muratoreanu, G. Statistical Analysis of Heavy Rains and Floods around the French Mediterranean Basin over One Half a Century of Observations. *Geosciences* **2022**, *12*, 447. <https://doi.org/10.3390/geosciences12120447>

Academic Editors: Andrea Gioia, Pedro Pinto Santos and Jesus Martinez-Frias

Received: 1 October 2022

Accepted: 1 December 2022

Published: 4 December 2022

Publisher's Note: MDPI stays neutral with regard to jurisdictional claims in published maps and institutional affiliations.



Copyright: © 2022 by the authors. Licensee MDPI, Basel, Switzerland. This article is an open access article distributed under the terms and conditions of the Creative Commons Attribution (CC BY) license (<https://creativecommons.org/licenses/by/4.0/>).

1. Introduction

Global warming is increasingly confirmed in all regions of the world. In France, 2020 is regarded as a record year as the average temperature of 14 °C has, since the beginning of meteorological record-keeping, never been observed [1]. It thus joins the hottest 10 years recorded in the 21st century (2018, 2014, 2019, 2011, 2003, 2015, 2017 and 2006). If the year 2021 turned out to be less hot, during the summer of 2022, the temperatures recorded were marked by an intensity never equaled. It is the second hottest summer observed in France since at least 1900 with a difference of +2.3 °C compared to the 1991–2020 average (summer 2003 remains the hottest ever measured in France with a temperature anomaly of +2.7 °C). According to NASA, the global thermal anomaly for the period from June to August 2022 has reached an all-time high since records began in 1880. While global warming affects a very large portion of the planet in a more or less homogenous manner, rainfall evolution is nevertheless marked by significant regional disparities. However, given the rise of temperatures and air evaporation power, an increase in precipitation is likely in some parts of the world. Ref. [2] claims that an increase in water vapour in the lower layers of the atmosphere may also be the cause of an increase in precipitation and of their heavy nature. In 2010, [3] attested to a slight increase in centennial rainfall. Other authors [4–6] have also confirmed a weak but not significant upward trend of heavy precipitations in the same region. As part of the ANR/Extraflo project, [7] came up with the same result according to a daily time step for more than 900 climate series. Climate changes are expected to influence the time and intensity of floods caused by the water network in Europe [8].

Better known as Mediterranean episodes or Cévennes episodes (rainy episodes with intensities greater than 100 mm/24 h), these intense rains can sometimes be accompanied by violent winds, hail and often they are the cause of major flooding and flash floods. The

choice of a rainfall intensity threshold to study them statistically has been dealt with by several studies. Indeed, how can one describe this parameter, taking into account global climate diversity? How can these thresholds be defined according to society's perception being applied to the hazard scale? In 2013, [9] extensively revisited this issue and this value applied by scientists to rainfall in several areas of the world. In 2015, [10] also evoked this notion and its spatial perception; [11] showed in a study on the evolution of intense rainfall in the French Mediterranean region a trend towards the intensification of these phenomena between 1965 and 2015 (+22% on the annual maxima of daily accumulations and an increase rainfall frequencies of more than 200 mm/24 h). Ref. [12] also arrive at a similar result with an average increase in intensity of +22% (+7 to +39% at the 90% confidence level) over the period 1961–2015. According to IPCC [13], the projected increase in the intensity of extreme precipitation will result in an increase in the frequency and magnitude of pluvial floods—surface water and flash floods (at a high level of confidence) (the floods storms result from rainfall intensity exceeding the capacity of natural and artificial drainage systems) [14]. According to this latest report, it is also very likely that episodes of heavy precipitation will intensify and become more frequent in most regions affected by significant global warming. Globally, extreme daily precipitation is projected to intensify by about 7% for every additional 1 °C (high confidence). Thus, for 1.5 °C more, the events (intense rain over a day) which occurred over a decade, will increase compared to the period (1850–1900) with a frequency of +1.5 more (while the atmospheric humidity will increase by +10.5%). If the warming reaches +4 °C, the increase in intense rainfall will be 2.7 times higher, while atmospheric humidity will be multiplied by 3 (30.2%).

The increase in floods in Europe has forced member countries to put in place the “Floods Directive” (2007/60/EC) with the aim of reducing the damaging consequences of floods. This charter establishes a common working method on a European scale (plan for management, protection and prevention of this type of risk) and imposes a timetable, including a review cycle, every six years. Although research on floods and their consequences is abundant, research on exposure to this type of risk remains scarce. For example, we cite the research carried out in Greece [15], the aim of which is to prioritize flood-prone areas according not only to the extent of the flood-prone cover, but also to the types of infrastructure that may be affected. Similar studies were also carried out in the USA [16], on the exposure of critical infrastructures to floods with a return period of 100 years, by combining the flood maps of the FEMA (Federal Emergency Management Agency) and the National Structure Database of the United States Geological Survey (USGS). There is also research undertaken in France, including [17], which is devoted to the exposure and social vulnerability of cities. The methodologies used in these different works are based on the crossing of several databases and the production of cartographic summaries. Despite the relevance of this work, they nevertheless remain linked to the limits of the definitions of thresholds and their application in the context of spatial distribution on a map. In 2021, 62.46% of catastrophic events worldwide involved floods. This figure represents an increase of +137% compared to the average for this type of phenomenon observed between 2001 and 2020 [18].

In France, floods are the main natural hazard. The areas neighbouring the Mediterranean Basin represent 80% of the cost of natural disasters. Despite one of the most efficient flood prevention and management systems in the world, each year these disasters generate huge human and material costs (in October 2018, 15 people died and 99 were injured in the department of Aude; in 2019, in the Béziers region, a similar event of lower intensity resulted in one death and significant material damage). Finally, more recently, in 2020, in Alpes-Maritimes, 26 people died following an exceptional event (locally, rainfall totalled over 500 mm/24 h in Saint-Martin-Vésubie). Each year, the Mediterranean episodes lead to significant human and material losses. In an analysis on mortality linked to intense rains in four Mediterranean areas (in Spain, Italy, Greece and throughout the French Mediterranean area) [19] showed that French regions observed the highest number of deaths and the most important fatal events between 1980 and 2015. In 2022, [20] extended this database

to a Euro-Mediterranean limit FFEM-DB. It now encompasses data for 2875 flood deaths from 12 territories (nine of which represent entire countries) in Europe and the wider Mediterranean region from 1980 to 2020.

2. Study Area, Data and Method

2.1. Study Area

The study area refers to the French Mediterranean region, which covers an area of 50,000 km² (just over 2% of the Circum-Mediterranean area) (Figure 1). This situation, described as marginal a few years ago [8,21–27], is likely to evolve and expand this climate range to the northern-most latitudes, given current climate changes. The seasonal rainfall model is one of the parameters which identify this climate within the complex typology of climates on the planet. With a short dry season concentrated in the summer months and a rainy season expanding from autumn to winter, depending on the subregions, there may be either an autumn or a winter maximum [28–33]. These conditions are the first climate classification criterion of the already mentioned climate area. The thermal parameter (warm summer and mild winter) is the second classification criterion.

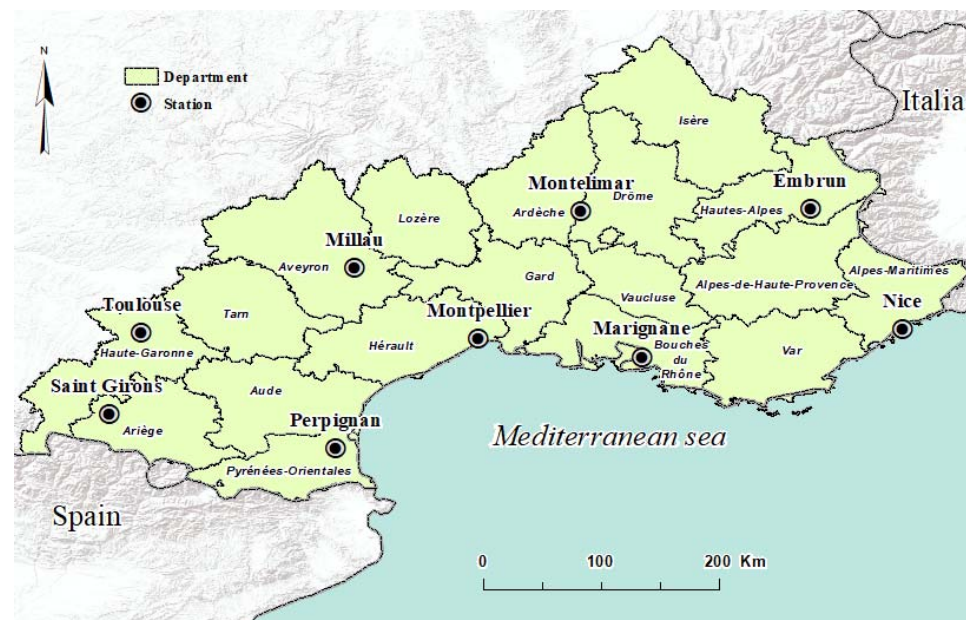


Figure 1. The locations of stations and departments in the study area.

2.2. Data

2.2.1. Data of Mediterranean Episodes (1968–2020)

The data regarding the Mediterranean episodes (a precipitation episode exceeding the threshold of 100 mm of rainfall in 24 or 48 h) used for this study come from the climatological Database of Météo-France (BDCLIM (<http://pluiesextremes.meteo.fr/france-metropole/-Evenements-memorables-.html>) (accessed on 15 March 2022) (2020).

We use observation frequency for each class by 18 departments (Figure 1):

- Class (100–200 mm), class (200–300 mm), class (>300 mm)/24 h
- Class (300–400 mm), class > 400 mm/48 h

2.2.2. Data of Rainfall and Temperature (1973–2020)

Total monthly rainfall and temperatures for 9 stations (Figure 1)

Total monthly rainfall amounts and temperatures (Tn and Tx) were collected by the NOAA Climate Data website (<https://www.ncdc.noaa.gov/data-access> (accessed on 15 March 2022)). They cover 9 stations over a period of 50 years of measurements (1973–2020).

2.2.3. Data of Flood

Frequency for each event.

The flood study relies on the data published by the Dartmouth Flood Observatory (<https://floodobservatory.colorado.edu/Archives/index.html> (accessed on 22 March 2022)) and the international disaster database (<https://www.emdat.be/> (accessed on 22 March 2022)). The observation period spans from 1988 to 2020.

2.2.4. Other Data

- The North Atlantic Oscillation (NAO) data are obtained as a monthly time-series from: <https://climexp.knmi.nl/selectdailyindex.cgi?id=someone@somewhere> (accessed on 22 March 2022).
- The Mediterranean Oscillation Indices (WeMOi), obtained from the normalized pressure difference between Padua and Cadiz, monthly. The monthly time-series are obtained from: https://crudata.uea.ac.uk/cru/data/moi/Web_WeMOi-2020.txt (accessed on 22 March 2022)
- SST data (for the Mediterranean Sea) (time series of sea surface temperature anomalies) ($^{\circ}\text{C}$), referring to the mean temperature between 1981 and 2010, in each of the European seas and in the Planetary Ocean). Data sources: SST data sets from Met Office (HadISST1, HadSST.4.0.0.0 și OSTIA), US National Ocean and Atmosphere Administration (ERSSTv5), ESA SST CCI analysis version 2.1. <https://www.eea.europa.eu/data-and-maps/figures/decadal-average-sea-surface-temperature-3/> (accessed on 22 March 2022).

3. Methodological Approach

- To study the spatial distribution and the evolution of Mediterranean episodes, we use an observation frequency analysis.
- The analysis of correlation between the index of climate “NOA”, “WMOI”, the temperature of the Mediterranean sea “SSTMED” and rainfall signal was computed by the coherence diagram (WCO) for different modes of variability.

To compare the time series with each other, cross-correlation analysis is used.

By analogy to the spectra crossed by Fourier transform, the spectrum in crossed wavelets is a method which makes it possible to evaluate the correlation between two signals according to the various scales (frequencies) during time [34–36].

The spectrum by crossed wavelets $W_{xy}(a, \tau)$ between two signals $x(t)$ and $y(t)$ is calculated according to the equation below, where $c_x(a, \tau)$ and $C_y^*(a, \tau)$ are the wavelet coefficient of the continuous signal $x(t)$ and the conjugate of the wavelet coefficient of $y(t)$, respectively:

$$W_{xy}(a, \tau) = c_x(a, \tau) \times C_y^*(a, \tau) \quad (1)$$

Continuous wavelet coherence can be defined as the estimate of the temporal evolution of linearity and of the relationship between two signals on a given scale [37–39]. Wavelet consistency is calculated using smoothed wavelet spectra of the $SW_{xy}(a, \tau)$ and $SW_{yy}(a, \tau)$ series and a smoothed crossed wavelet spectrum $SW_{xy}(a, \tau)$ [40]:

$$WC(a, T) = \frac{|SW_{xy}(a, \tau)|}{\sqrt{[|SW_{xy}(a, \tau)| \cdot |SW_{yy}(a, \tau)|]}} \quad (2)$$

Consistency is defined as being the modulus of the crossed spectrum normalized of the same spectrum having values between zero and one and represents the degree of linear between two processes. A value of 1 means a linear correlation between the two signals at a time T on the scale a and a value of 0 that indicates a zero correlation [37,40–42].

4. Results

The Mediterranean episodes and flood evolve over more than half a century of observation (1968–2020)

- Spatio-temporal variability of Mediterranean episodes

None of these events represent the same climatic phenomenon which favour the occurrence of heavy rainfall generated either by active rain depressions or by localized storm cells. When one refers to the Cévennes region and, more precisely, to the southern slopes, reference is made to this latter area. When one refers to the entire Mediterranean territory in the south of France or only a part of this area, it is called a Mediterranean episode. In 2016, [43] addressed this semantic issue, designating the same climatic process. One may even notice an overlap of the two episodes during the same weather event. According to [1], the annual frequency of such events is estimated to be between 3 and 6 episodes per year in Mediterranean regions. The spatial distribution of this phenomenon in the French Mediterranean area points to a central area which is highly exposed to this risk (Figure 2). In the three departments of Ardèche, Gard and Hérault, more than 39% of the most intense episodes were observed between 1990 and 2019. If we add Lozère, we reach 47% of these phenomena (which strengthens the role of the relief). Alps-Maritime, Var and Pyrénées-Orientales are the other departments with a high frequency of these phenomena, reaching almost 17% in all these three regions.

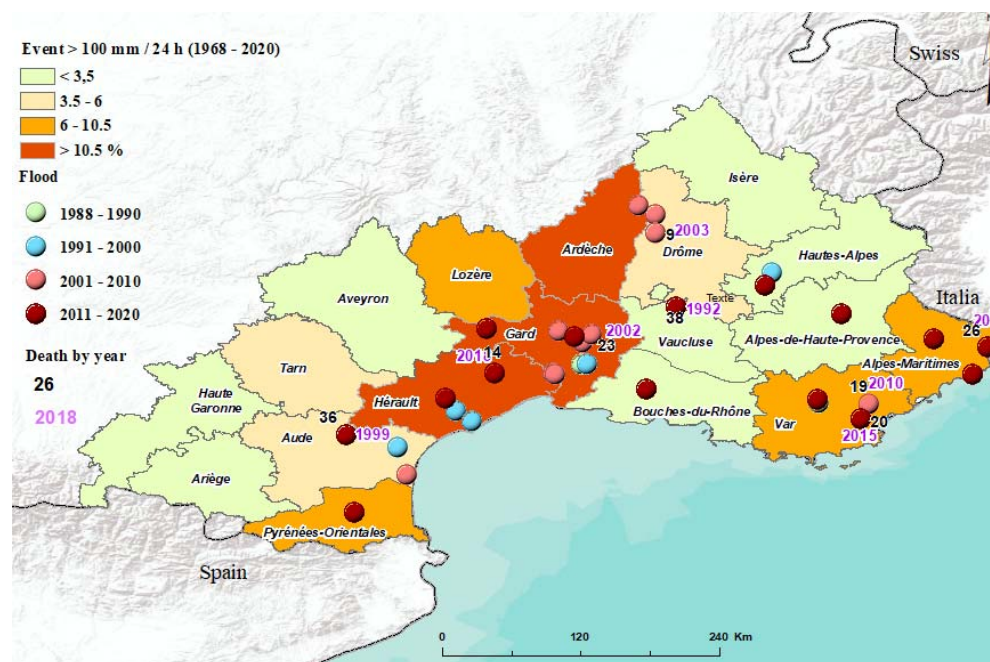


Figure 2. Heavy rainfall and floods in the French Mediterranean area. Data source: <http://pluiesextremes.meteo.fr/france-metropole/-Evenements-memorables-.html> (accessed on 15 March 2022). <http://floodobservatory.colorado.edu/Archives/index.html> (accessed on 22 March 2022).

In the French Mediterranean area, heavy rainfall is a recurrent phenomenon (Cévenol episode or Mediterranean episode). Each autumn, these phenomena cause several floods. In order to manage this danger, Météo-France set up a vigilance system (based on forecast and prevention) in 2001. This alert system informs the population, public authorities and emergency services about the imminence of a potential flood hazard 24 h before its occurrence. Following the terrible disasters in Vaison la Romaine (1992) and Gard (1999), the warning system developed with the establishment, in 2003, of the central service of support to flood forecasting (SCHAPI). This structure provides hydrometeorological surveillance (24 h a day) over all waterways in the French national territory and draws up

the flooding alert map within the “Vigicrues” (<https://www.vigicrues.gouv.fr/> (accessed on 24 March 2022)) system. In 2011, a new service was added to this network, namely APIC, a warning service for heavy rainfalls at the municipal level (a service set up by Météo-France which issues warnings and notifications in case of potentially dangerous precipitations). In 2017, a new service for flash flood warnings was created (Vigicrues Flash—a system of notification in the event of an exceptional hydrological forecast). This mobilization for warning and hazard management points to the complexity of this weather phenomenon whose consequences are harmful every single time. The map (Figure 2) drawn based on the statistics of hydrological events (floods) affecting the Mediterranean area between 1988 and 2020 shows the importance of this phenomenon in this region. All departments located on the coast are affected by this type of hazard. Also, one should note a vulnerability of central areas (the Cévennes) and of the Prealps in the east. Chronologically, the floods of the last two decades (1991–2000 and 2001–2010) affected the central and “western” areas much more. Over the past decade (2011–2020), these phenomena spread to the ‘east’ of the French Mediterranean area. Furthermore, we notice that this period stands out through a higher frequency of these events (16 episodes as compared to 10 in the 2001–2010 decade, which means an increase of almost 60%). Between the 1991–2000 decade and the most recent decade, the progression reached 167%.

This dramatic increase in events is probably related to the effects of climate changes and particularly to the recurrence of extreme weather events. Looking more closely at the consequences of floods on human society and their causes, one can note that:

- The largest number of deaths are recorded in the last decade (104 deaths in 2011–2020) (Table 1).
- The largest number of episodes of heavy and torrential rains are to be observed in the same decade (14 episodes of heavy rains and 4 of torrential rains) (this proves what we have previously mentioned regarding the increase in extreme phenomena associated with climate changes).

Table 1. Deaths caused by floods in 1991–2020 in the French Mediterranean area. Source: <http://floodobservatory.colorado.edu/Archives/index.html> (accessed on 22 March 2022).

Period	Number of Floods	Deaths	Number of Episodes Heavy Rain	Number of Torrential Rain Events
2011–2020	16	104	14	4
2001–2010	10	62	7	3
1991–2000	6	87	5	1
Total	32	253	20	8

The map also shows that the most dangerous episodes may target the departments in which heavy rains are less frequent. This confirms the fact that these episodes are focused on certain regions (38 deaths in Vaucluse in 1992, 36 deaths in the department of Aude in 1999 and 26 in Alpes Maritimes in 2020).

- Mediterranean episode trends in the 18 departments (1968–2018)

The curves resulting from centred-small deviations of observation frequencies of heavy rainfall episodes for the 1968–2018 period allow the identification of vicissitudes that marked this climate parameter throughout this very long period of observation.

The frequency analysis will initially cover the 100–200, 200–300 classes and classes higher than 300 mm within 24 h (Figure 3a–c).



Figure 3. Centred-small deviations of annual observation frequencies of rainy days with intensities above 100 mm in 24 h in the 9 departments of the Mediterranean area (1968–2020) ($RI = (X_i - X)/S$, where X_i is yearly value, X is the series average and S is standard deviation).

For the first class 100 to 200 mm, the trend curve (moving average over 5 years) makes it possible to identify four distinct periods (Figure 3a).

From 1968 to 1979, there is an upward trend and the annual value curve points to eight years with a positive index as compared to four years in which the centred-reduced index is negative. The values are marked by two very large centred reduced deviations

recorded in 1972 (+1.3) and 1976 (+1.9). These values contrast with the poor ones observed during the rest of the years of this 12-year period which do not exceed + or -0.6 .

From 1980 to 1992, the decrease in values prevails (10 years have a negative index, four of which have values higher than -1 and one reaches -2.4 in 1985). Only four years have a positive centred-reduced deviation which reached $+0.5$ in 1987, its maximum positive value.

From 1993 to 2003, the trend changes and there is an increase in intense phenomena. Positive indices are predominant. There are five years with a difference over $+1$ (1994, 1996, 2000, 2002 and 2003). Three years have negative indices. In 1998 and 2001, the centred-reduced deviation exceeds -1 and falls below this value in 2004.

From 2004 to 2020, the trend marked by the curve is stable, but there is a pronounced interannual variability. Thus, a shift from a positive to a negative year occurs, namely between 2007 and 2008 when there is a switch from -1.7 to $+0.86$. As regards the following years, one notes that the positive years are more pronounced, indicating more extreme events (2011 and 2014 have an index which is over $+1$, whereas 2018 records only $+1$). Furthermore, one should see that this last cycle has a sequence of two–three years with a negative index which is interposed between the positive years.

The 200–300-mm class (Figure 3b) is analysed in the same manner. This makes it possible to detect remarkable fluctuations due to the analysis of centred-small index curves. The number examination leads to identifying three major periods of fluctuations: From 1968 to 1991, there is a stable trend, but one which is marked by less intense events in this class of precipitations. This confirms the importance of years with negative indices noted in this period (15 years, four of which have values higher than -1 , 1974, 1975, 1978 and 1981). At the same time, there are six years distributed throughout this cycle, with positive values reaching $+2$ in 1977 and $+1.2$ in 1988.

The 1992–2006 period is highly marked by rainy episodes of this class. The increase in values is to be observed over ten years (positive indices) and is also marked by the recording of centred small deviations over several successive years that exceed $+1$ (1994, 1995, 1996, 1997, 1999 and 2003).

From 2007 to 2020, a general downward trend appears on the graphs. The number of events in this rain class only increased significantly in two years (2011 with $+0.89$ and 2014 with $+1.76$); we also note five years with negative indices below -1 (2007, 2008, 2009, 2012, 2013, 2017).

The >300 -mm class (Figure 3c)

From 1968 to 1991 we note the same evolution as that described above, but the trend remains more stable. Only two years stand out with significant indices, 1980 with $+1.56$ and 1982 with $+2.57$. Between 1992 and 2002, the episodes of rain of this class are more numerous and the years with positive index predominate.

From 2003 to 2007, there is a relatively calm period (less rainfall with accumulation higher than 300 mm). This is not the case for events of lower precipitation classes (although, in terms of the previously discussed classes, 100–200 and 200–300, the number of rainy episodes observed decreases as compared to the total of the period studied).

From 2008 to 2020, extreme events become recurrent. This is highlighted by the number of years with a positive index (9) compared to 4 (negative). 2014 sets a record for the studied series with an index reaching $+3.24$. Finally, in the last seven years, events of heavy rainfall over 300 mm regularly exceed the average for the studied series, except for 2017.

Analysing Figure 3d,e, featuring the 48-h interval (of the largest rainfall accumulations between 300 mm and 400 mm and higher than 400 mm), one can note roughly the same fluctuations (except the first cycle). The four phases studied are present, but with slightly different time amplitudes.

As regards the 300–400-mm range (Figure 3d):

From 1968 to 1991, the moving average curve calculated over five years shows an upward trend in observing these phenomena. Seven years record a positive index, two

of which with a value over +1.5 (1970 and 1976). The years with a negative difference are more numerous (16 years), five of which are above 1.

From 1992 to 1997, this precipitation cycle is marked by a higher rainfall frequency, the 24-h accumulation of which is between 300 mm and 400 mm. The uninterrupted succession of positive years in this cycle is to be noticed. Furthermore, one should see that the index exceeds +1 in 1994, 1996 and 1997.

Between 1998 and 2009, the period is less favourable to observing extreme phenomena (rainfall accumulation exceeding 300 mm in 48 h).

From 2010 to 2020, we should note a recurrence of heavy rain episodes (seven positive years and four negative years). 2014 stands out through a positive index of +2.4.

In terms of the >400-mm class (Figure 3e):

The analysis of events related to this class reveals two distinct phases:

Between 1968 and 1993, there are two years with significant indices, 1968 (+1.18) and 1982 (+2.59). Moreover, one should note the large number of years with negative indices, thus mentioning the low frequency of these events in this period.

From 1994 to 2020, observations of days with 48-h cycles of heavy rain exceeding 400 mm point to a significant increase in these events. However, this phenomenon does not affect every year in the above-mentioned time span. Thus, positive years are, more often than not, followed by one, two or three years with a negative index. The last extraordinary point of this analysis is, without a doubt, the remarkable increase in observation frequencies over the years (1997, 2008, 2011, 2014 and 2020 with 2.12, 2.59, 2.12, 2.59 and 1.65).

The analysis of heavy rainfall evolution recorded in the Mediterranean departments, depending on the various precipitation thresholds observed in 24 or 48 h, indicates an increase in the last years of the series under study. We should also note that high intensities (between 300 mm and 400 mm and over 400 mm) are the most present. The period (1992–2003) is a cycle in which these phenomena were the most recurrent. Lastly, at the beginning of the chronological series (1968–1991 to 1993), these phenomena are less observed (moving average curves show a stable evolution with a more pronounced downward trend).

5. Discussion

5.1. The Link between the Increase of Intense Events and Global Warming

One of the climate change consequences is, without a doubt, the increase in extreme phenomena [21,44–49] in the study area. Here we have noticed increased temperature due to global warming intensity in the last decade. Thus, Table 2 sums up the average temperatures over ten years for the entire region. It shows that, in the last decade, the highest values were recorded in the French Mediterranean area. The difference between decades D and A is assessed at +1.13°C and rises to +1.68 °C for Tx for the same periods (Table 2). This last hot decade thus coincides with a sharp increase in Mediterranean episodes. The difference between the decades (2011–2020) and (2001–2010) points to a rise of +11.59% for thresholds >300 mm in 24 h and an increase of almost 10% for thresholds above 400 mm in 48 h (“Tx” stands for maximum temperatures recorded during the day; this rise in episodes might be explained by a greater number of storms observed in the region). An unprecedented increase in severe floods occurred in the area (16 floods and 104 deaths were observed in the last decade, these being the highest numbers and the highest balance in the studied series) (Table 1). This suggests a strong connection between the two phenomena under study (this connection cannot be considered direct but remains in line with the trend observed worldwide in the last years). Also, the role of the human factor in the occurrence of floods and in the scale of severity of these phenomena is evident.

Table 2. Mean temperature over 10 years and difference between decades (2020–2011, A; 2010–2001, B; 2000–1991, C and 1990–1981, D).

Decade	T	Tx	Tn	Decade	T difference	Tx Difference	Tn Difference
A	15.79	21.64	9.97	A-B	0.50	0.82	0.20
B	15.29	20.82	9.76	B-C	0.01	0.02	0.00
C	15.28	20.80	9.76	C-D	0.62	0.82	0.42
D	14.66	19.98	9.34				

Figure 4 shows the evolution of maximum temperatures. We note on this chart that the onset of warming is the year 1990 and the intensification of the cycle is around 2013. At the same time, the largest increase in Mediterranean episodes (>300 mm/24 h) is observed over the last global warming cycle (2013–2018 on the moving average curve).

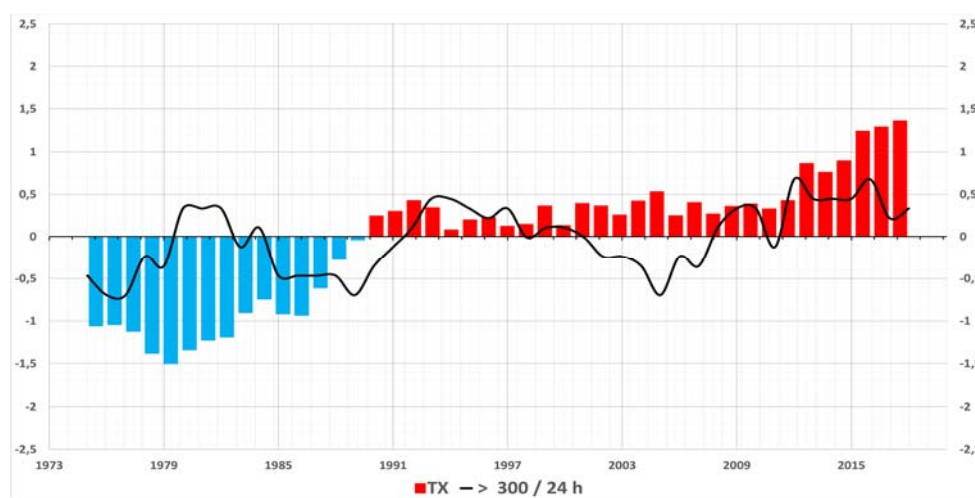


Figure 4. Evolution of centred small deviations of Mediterranean episodes (higher than 300 mm in 24 h) and of regional averages of maximum temperatures (Tx) (five-year moving average) (1973–2020). ($RI = (X_i - X)/S$ -where X_i is yearly value, X is the series average and S is standard deviation).

5.2. The Link with Regional Patterns of Climate Variability

Real scientific progress in understanding climate change mechanisms worldwide has been made in the last years. This knowledge now makes it possible to state that climate is subject to natural fluctuations, coupled with a number of anthropic signals. The role of oceans in regulating convective flows has been extensively studied [50–55]. Climate fluctuations at middle and high latitudes are characterized by well-defined patterns or variability modes which, on a larger scale, point to a strong spatial cohesion. Thus, due to the study of pressure fields and ocean temperatures during the 20th century, two natural signals have been identified; they are known as multi-decadal signal (a recurrent signal over more than 40 years, with high frequency variability) and almost decennial (a signal with a short periodicity of 8 up to 14 years and low frequency variability) [56–58].

5.2.1. Link with NAO

In the Atlantic Ocean basin, the dominant atmospheric mode is the North Atlantic Oscillation (NAO). Its influence extends across the North Atlantic and even affects climates of the Mediterranean basin, North Africa and the Middle East. The NAO is an alternation of atmospheric mass between the arctic and subarctic regions and the subtropical regions of the Atlantic. The surface pressure field at sea level is used to describe this oscillation. The positive phase corresponds to a strengthening of the two action centres (the deepening of the Icelandic low, the development and intensification of the Azores High). In this phase, there is a strengthening of the meridian pressure gradient over the Atlantic (the prevailing

westerly winds increase in winter beyond 45° N and the alignment of depressions moves northward); the French Mediterranean area is thus subject to a greater drought. The negative phase is observed when these centers weaken simultaneously. The development direction is pushed southwards and the Mediterranean area is subject to weather events consisting of thunderstorms and precipitations.

The Figure 5 shows the moving averages calculated for the NAO index (monthly average index calculated for September, October and November of every year, a period favouring the occurrence of such events), and the intense rains (annual cumulative rainfall > 100 mm/24). We note the close connection observed in the 1993–1995 period until 2003–2005 (inverse relationship, negative phase of index NAO and positive index for the heavy rain). This period has been characterized by a sudden increase in the frequency of these phenomena (Figure 3).

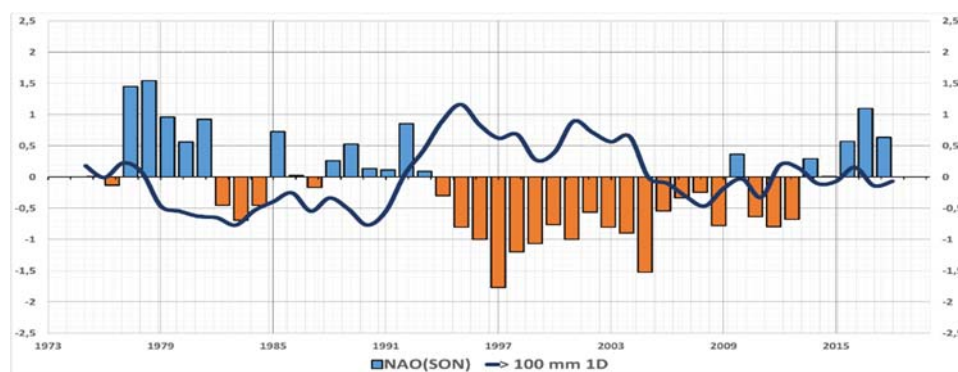


Figure 5. The evolution of centred small deviations of Mediterranean episodes (higher than 100 mm in 24 h) and of NAO indices for September, October and November (five-year moving average) (1973–2020) ($RI = (Xi - X)/S$ -where Xi is yearly value, X is the series average and S is standard deviation).

To delve into this analysis, we shall employ the wavelet coherence method in identifying the relationships which may exist between regional rainfall (monthly average of the nine observation posts under study and the various variability modes of the NAO). The data of Mediterranean episodes are structured by departments and by the number of observed events. These data may be used only on an annual basis, as the results obtained by this approach are inconclusive. We have therefore preferred the monthly rainfall data recorded in the nine studied stations. The NAO shows a coherence essentially distributed from the interannual scale to the decennial scale. The annual cycle (Figure 6A) is proved for the entire period, but one may note a number of significant consistency losses (between 2000 and 2010). There is a strong coherence on the energy band 2–4 years (mid-80s–mid-2000s). It correlates with the phase of increase in intense phenomena (noticed during the frequency study in Figure 3). The percentage coherence calculated for this band is almost 73% (Figure 6C). We found this coherence expressed for the energy band 4–8 years with a coefficient of 72.30% (Figure 7A–C). On the ten-year scale, the 8–12-year band is expressed by the strong coherence calculated with NAO (almost 82%) (Table 3 and Figures 5 and 6A). However, this is stronger at the beginning of the period before 2000. Finally, the coherence over the last period of the series under study is more pronounced in the 8–12-year energy band and in the annual 1–2-year band (Figure 6A–C).

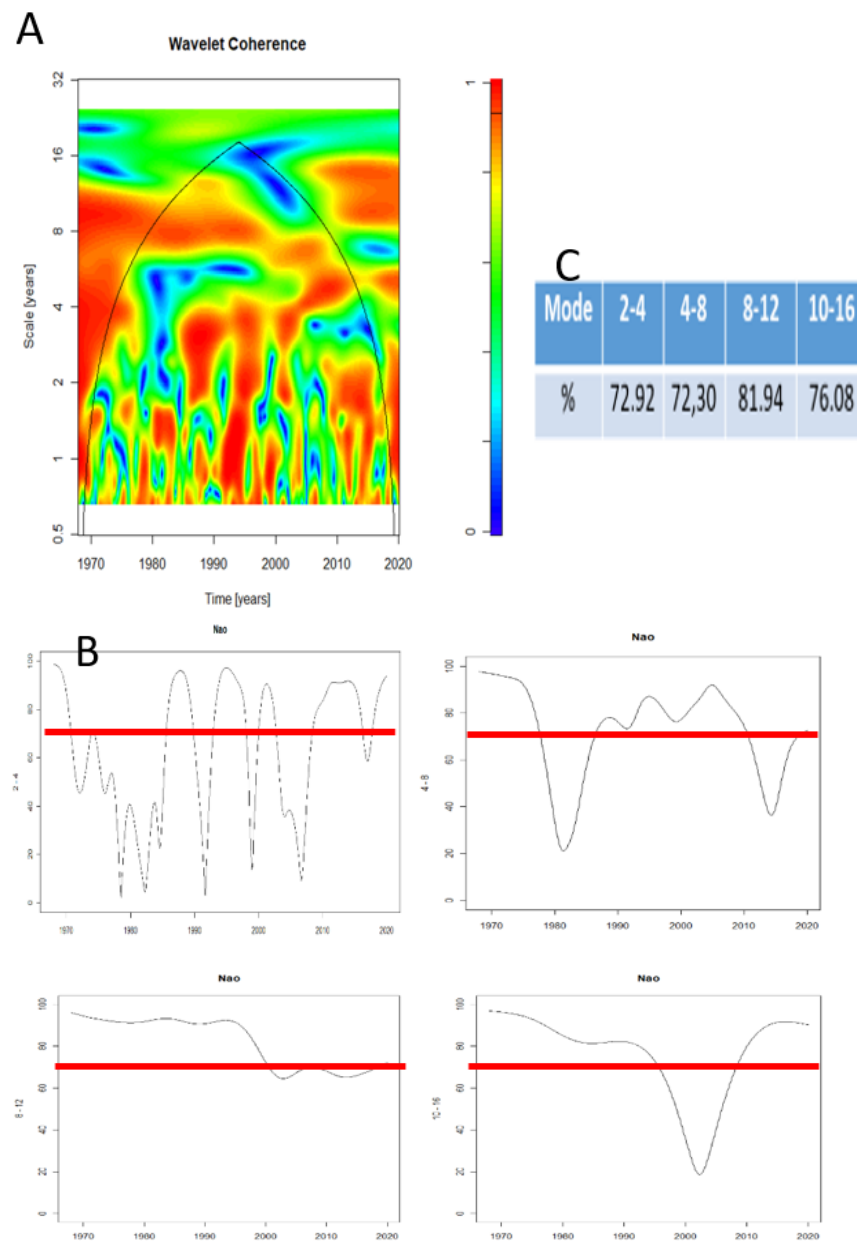


Figure 6. (A)—Wavelet correlation between regional monthly average precipitation and annual NAO index. (B)—Wavelet correlation between regional monthly average precipitation and annual NAO index depending on various modes of variability. (C)—Wavelet correlation (in %) between regional precipitation and NAO index (percentage) (1968–2020).

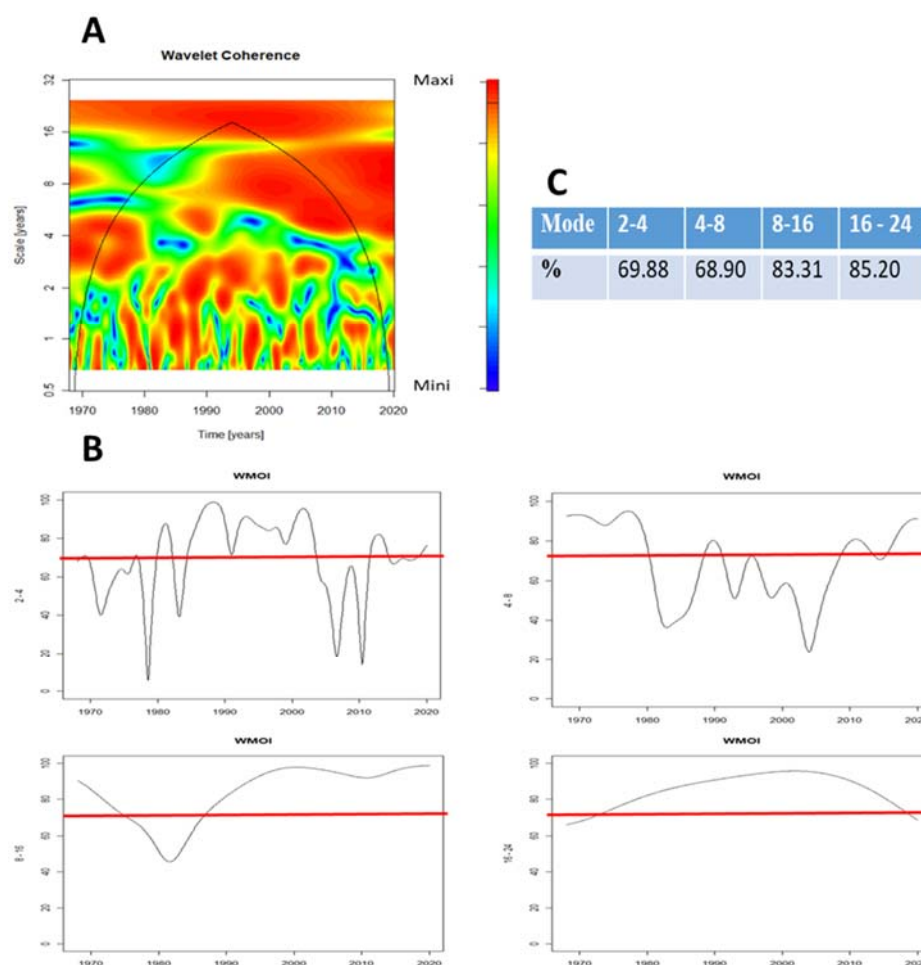


Figure 7. (A)—Wavelet correlation between regional monthly average precipitation and WMOI index. (B)—Wavelet correlation between regional monthly average precipitation and WMOI index depending on various modes of variability. (C)—Wavelet correlation between regional precipitation and WMOI index (percentage) (1968–2020).

Table 3. Synthesis of the research of correlations between local precipitation, NAO index, WMOI index, the Mediterranean Sea Surface Temperature (SSTMED) and the maximum air temperature (Tx).

Period	TX	NAO	WMOI	SSTMED
Period before 1991		Ten-year and multi-decadal 8–12 and 12–16 years	Interannual scale 4–8 years	Decadal and multi-decadal scale 16–24 and 16–32 years
Period 1991–2000	connection	Interannual scale 2–4 years and 4–8 years	Interannual and ten-year 2–4 years and 8–16 years	Interannual scale 1.5 to 3 years
Period 2011–2020	Evidence connection	Ten-year scale 10–16 years	Decadal and multi-decadal scale 8–16 and 16–24 years	Interannual scale 1.5 to 3 years

5.2.2. The Link with the Local Atmospheric Circulation

In the Mediterranean area, the climate also depends on air-sea exchanges (latent and sensible heat). Refs. [57,59] have suggested the potential existence of a Mediterranean oscillation (MOI and WMOI) as a consequence of the bipolar behaviour of the atmosphere between the western and eastern Mediterranean. The differences in temperatures, precipitations, circulation and other parameters between the two basins have been attributed to these oscillations [60]. The MOI index used to measure this variability pattern is calculated based on the difference in atmospheric pressure between Alger and Cairo, between Israel

and Gibraltar and for the WMOI between Padua and Cadiz. Thus, in a positive phase, the Mediterranean region is subject to a greater drought. In the negative phase, the conditions are humid.

The use of wavelet coherence makes it possible to assess and describe the connections between rainfall and climate variability in the Mediterranean area (represented by the WMOI index, in a first stage the pressure difference between Padua and Cadiz and, in a second stage, SSTMED—the Mediterranean Sea surface temperature) both for the various scales (frequencies) and in terms of the evolutions of relations in time.

Connection with WMOI

Annual cyclicity is expressed throughout the period, but with significant consistency losses. A correlation is observed on the 2–4-year energy band. It does not appear to be continuous between 1968 and 1980 and in the mid-eighties and early 2000s. This last phase displays the strongest correlation percentage, which is over 70% (Figure 7A,B). In terms of the 4–8-year band, on the other hand, a maximum of energy may be noticed at the beginning and the end of the period under study. Lastly, for the 10-year scale (8–16) and the multi-decadal scale (16–24 years), the correlation is very strong and exceeds 80% (Figure 7C). For the first annual band, the correlation is very strong between 1990 and 2020. For the second energy band, it is better expressed between 1998 and 2015 (Figure 7A,B).

Connection with the Mediterranean Sea surface temperature

Given the current climate change, a sea level rise and an increase in the Mediterranean Sea surface temperatures are expected. Following a study of satellite data AVHRR (Advanced Very-High-Resolution Radiometer) conducted over a period of 24 years (1985–2008), a sudden increase in surface temperature with an intensification in the 1980s was detected. This increase was quantified at $+0.24$ °C per decade between 1986 and 2015. In 2017, [61] calculated the temperature rise at $+0.4$ °C/decade for the same measurement period. Other studies also suggest an increase in this parameter [5,62–64]. Considering the results of current research (carried out based on the current trend and projections for the future), an increase in the Mediterranean Sea temperature is to be expected in the years to come. Furthermore, this vast almost closed intercontinental sea is a huge water reservoir (only the Strait of Gibraltar provides water exchange with the Atlantic Ocean). This parameter is the first factor (the heat and moisture uptake of air masses) in the development of Mediterranean episodes observed in the south of France. The second factor is materialized through the interaction between the air masses from the south and the cold air coming from the altitude (which begins to have a pronounced meridian trajectory during this period).

The analysis of correlations between the Mediterranean SST and the average regional precipitation has made it possible to prove that, on an annual scale, there is a weak relation between precipitations in the Mediterranean area and the Mediterranean Sea surface temperature (Figure 8). However, there is a high energy section in the band (1.5–3 years). This is confirmed between 1980 and 1990 and also between 2005 and 2015 (more intense for this latter period with correlations well over 70%) (Figure 8A). As regards the 4–8-year energetic band, the correlation is established at over 68% (Figure 8C). This was more intense between 1968 and 1980 (Figure 8B). The strongest correlation is that expressed by the multidecadal scale (16–24 and 16–32 years) in Figure 8C. Still, this seems to be more convincing between 1968 and 1990.

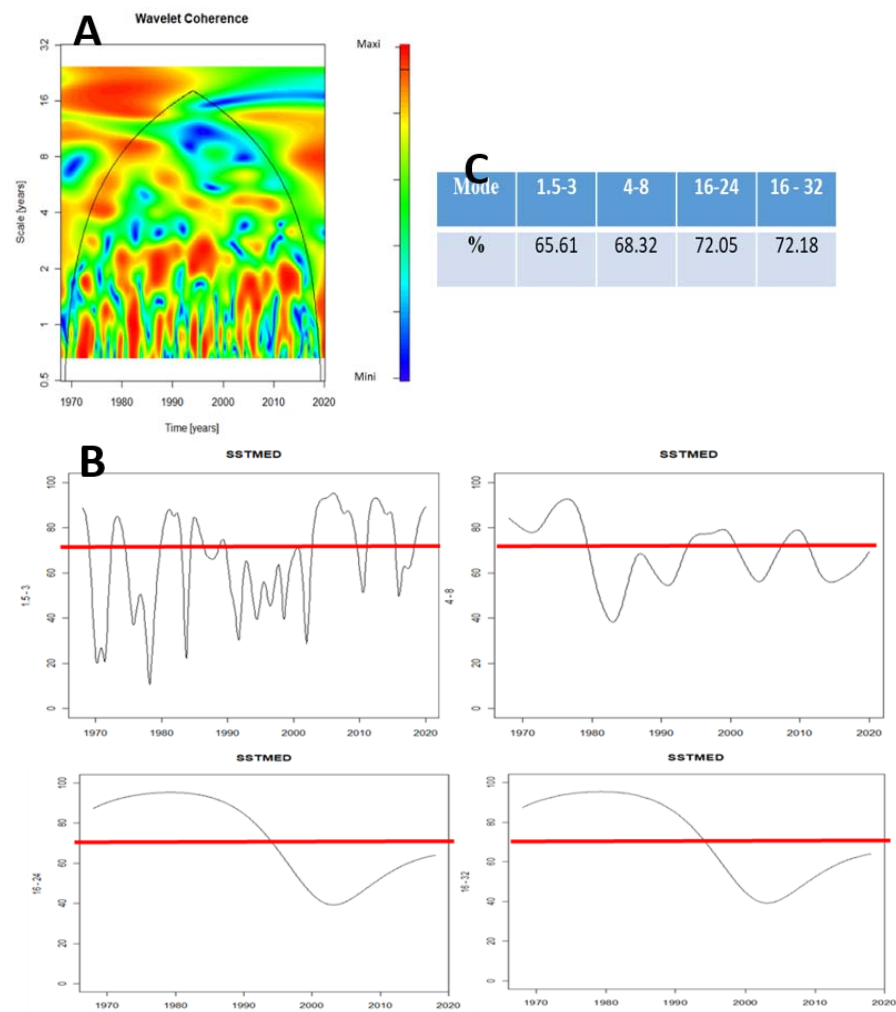


Figure 8. (A)—Wavelet correlation between regional monthly average precipitation and the Mediterranean Sea Surface Temperature (SSTMED). (B)—Wavelet correlation between regional monthly average precipitation and the Mediterranean Sea surface temperature (SSTMED) depending on the various modes of variability. (C) – Wavelet correlation between regional precipitation and SSTMED (percentage) (1968–2020).

6. Conclusions

The Mediterranean episodes are climate phenomena characteristic of the southern regions of France. Because of the heavy rainfall events which occur during these episodes, they represent a high risk of flooding in terms of river floods and flash floods. The analysis of the frequency of intensity classes > 100 mm for 24 and 48 h has shown that this phenomenon mainly affects 4 departments: Gard, Hérault, Lozère and Ardèche. The current trend for 3131 events occurring over a period of just over 50 years (1968–2020) in the 18 departments under study is not significant in the long run (coefficient of determination $R^2 = 0.0018$).

Local precipitation is subject to local and regional atmospheric fluctuations. The search for correlations between Mediterranean episodes, climate variability, and increase in air temperature and in the Mediterranean Sea surface temperature has made it possible to highlight some convincing connections. These connections point out that the current climate change increases the probability of this type of phenomenon. The human factor remains important and decisive in the occurrence of floods and deluges resulting from this type of phenomenon. The synthesis of these connections is presented in Table 3—the influence Mediterranean Sea surface temperature occurs in low frequencies (decennial and multidecadal scale before 1991). After these time intervals, the influence of the sea can be observed particularly in high frequencies. The NAO influence is more pronounced in the

high frequencies of the 1991–2000 period and in the low frequencies for the other periods. The WMOI is marked by a strong correlation for the period 2011–2020 in low frequencies. Finally, during the last decade (2011–2020), there is a more intense correlation between daytime temperature (T_x) and the Mediterranean episodes.

Thus, the rains observed during these Mediterranean episodes are characterized by intensity, which often favours the onset of floods and inundations. If one admits that the influence of general and local atmospheric circulation is closely related to the pluviogenesis of these phenomena, the onset of floods and inundations is closely related to the topography and spatial planning.

The role of the relief (a trigger for heavy rainfall) is a fixed parameter, but it cannot be considered in terms of altitude only. The slope exposition, the existence of valley corridors which allow the channelling of air masses laden with moisture, are also important.

The second parameter is the degree of humanization. The area is characterized by high demographic pressure over the natural environment and accelerated massive urbanization. Between 1970 and 2000, the cultivated area of the 880 municipalities on the French coast decreased by 20%, i.e., a loss of 200,000 ha [6]. According to INSEE (the National Institute of Statistics and Economic Studies), 17.5% of the dwellings built in coastal areas in 2010 are located in potential flood-prone areas. Thus, the development and territorial extension of built spaces increase the degree of soil impermeability and implicitly a pronounced surface runoff. For example, in La Garde, in the department of Var, the population increased five times in 50 years. This spectacular progression is doubled by an exceptional urbanization growth, as shown in the photos below (Figure 9).



Figure 9. The evolution of urbanization between 1955 and 2017 in the municipality of La Grade (Var department). Source: https://www.francetvinfo.fr/meteo/inondations/intemperies-dans-le-sud-est/avant-apres-dans-var-l-urbanisation-galopante-aggrave-les-degats-causes-par-les-inondations_3727533.html (accessed on 30 March 2022).

Population density values are high in the French Mediterranean area. According to INSEE, 20% of the country population live in the “Provence–Alps–Côte d’Azur” region, which represents only 10% of the territory of France.

The combination of human and climate factors accounts for the large amount of material damage and human casualties observed in the past years in this highly vulnerable sector in southern France. The risk management and prevention systems, which are nowadays present in this region, are very efficient, and land use laws are very restrictive. However, it is not excluded that the next few years may be still marked by these disasters,

as the economic stakes are high and the efforts to mitigate the effects of climate change are limited.

In the field of adaptation and resilience to climate change and its impacts, new research dynamics in the context of flood-related risks must be understood according to a global systemic approach. This approach must integrate sustainable development on a larger scale. If the use of modeling can provide an answer in terms of return duration and intensity of the risks incurred, studies that integrate the spatial distribution of human settlements and their vulnerabilities must be preferred, despite their complexity, because often they give a tangible answer (feedback on experience). This makes it possible to better understand and fight against floods.

Author Contributions: Conceptualization, Z.N. and O.M.; methodology, Z.N. and O.M.; software, Z.N. and G.M.; validation, Z.N., O.M. and G.M.; formal analysis, O.M.; investigation, Z.N.; resources, Z.N.; writing—original draft preparation, Z.N.; writing—review and editing, Z.N., G.M. and O.M. All authors have read and agreed to the published version of the manuscript.

Funding: This research received no external funding.

Data Availability Statement: Not applicable.

Conflicts of Interest: The authors declare no conflict of interest.

References

1. Météo—France. 2019. Available online: <https://pluiesextremes.meteo.fr/> (accessed on 15 March 2022).
2. Boe, J. *Changement Global et Cycle Hydrologique: Une Étude de Régionalisation sur la France*. Ph.D. Thesis, Centre Européen de Recherche et de Formation Avancée en Calcul Scientifique (CERFACS), Université Paul Sabatier-Toulouse III, Toulouse, France, 2008.
3. Neppel, L.; Pujol, N.; Sabatier, R. A multivariate regional test for detection of trends in extreme rainfall: The case of extreme daily rainfall in the French Mediterranean area. *Adv. Geosci.* **2010**, *23*, 145–148. [\[CrossRef\]](#)
4. Cantet, P.; Bacro, J.-N.; Arnaud, P. Using a rainfall stochastic generator to detect trends in extreme rainfall. *Stoch. Environ. Res. Risk Assess.* **2011**, *25*, 429–441. [\[CrossRef\]](#)
5. Collins, M.; Knutti, R.; Arblaster, J.; Dufresne, J.-L.; Fichet, T.; Friedlingstein, P.; Gao, X.; Gutowski, W.J.; Johns, T.; Krinner, G.; et al. Long-term climate change: Projections, commitments and irreversibility. In *Climate Change 2013: The Physical Science Basis. Contribution of Working Group I to the Fifth Assessment Report of the Intergovernmental Panel on Climate Change*; Stocker, T.F., Qin, D., Plattner, G.K., Tignor, M., Allen, S.K., Boschung, J., Nauels, A., Xia, Y., Bex, V., Midgley, P.M., Eds.; Cambridge University Press: Cambridge, UK; New York, NY, USA, 2013.
6. Daligaux, J.; Paul Minvielle Stéphane Angles, S. Paysages de l'agriculture littorale dans le Var. *Méditerranée Rev. Géographique Des Pays Méditerranéens/J. Mediterr. Geogr.* **2013**, *120*, 87–98. [\[CrossRef\]](#)
7. Soubeyroux, J.M.; Neppel, L.; Veyssière, J.M.; Trambly, Y.; Carreau, J.; Gouget, V. Evolution des précipitations extrêmes en France en contexte de changement climatique. *La Houille Blanche* **2015**, *2015*, 27–33. [\[CrossRef\]](#)
8. Blöschl, G.; Hall, J.; Parajka, J.; A.P. Changing climate shifts timing of European floods. *Science* **2017**, *357*, 588–590. [\[CrossRef\]](#)
9. Groisman, P.Y.; Knight, R.W.; Zolina, O.G. Recent trends in regional and global intense precipitation patterns. *Clim. Vulnerability* **2013**, *5*, 25–55.
10. Harader, E. *L'impact du Changement Climatique sur les Événements Hydrologiques Extrêmes des Petits Bassins Versants Méditerranéens: Le Cas du Bassin Versant du Lez*. Ph.D. Thesis, Université de Toulouse, Université Toulouse III-Paul Sabatier, Toulouse, France, 2015.
11. Ribes, A.; Thao, S.; Vautard, R.; Dubuisson, B.; Somot, S.; Colin, J.; Planton, S.; Soubeyroux, J.-M. Observed increase in extreme daily rainfall in the French Mediterranean. *Clim. Dyn.* **2018**, *521*, 1095–1114. [\[CrossRef\]](#)
12. Trambly, Y.; Somot, S. Future evolution of extreme precipitation in the Mediterranean. *Clim. Change* **2018**, *1512*, 289–302. [\[CrossRef\]](#)
13. IPCC. Summary for Policymakers. In *Climate Change 2021: The Physical Science Basis. Contribution of Working Group I to the Sixth Assessment Report of the Intergovernmental Panel on Climate Change*; Masson-Delmotte, V., Zhai, P., Pirani, A., Connors, S.L., Péan, C., Berger, S., Caud, N., Chen, Y., Goldfarb, L., Gomis, M.I., et al., Eds.; IPCC: Geneva, Switzerland, 2021.
14. Seneviratne, S.I.; Zhang, X.; Adnan, M.; Badi, W.; Dereczynski, C.; di Luca, A.; Ghosh, S.; Iskandar, I.; Kossin, J.; Lewis, S.; et al. Weather and Climate Extreme Events in a Changing Climate. In *Climate Change 2021: The Physical Science Basis. Contribution of Working Group I to the Sixth Assessment Report of the Intergovernmental Panel on Climate Change*; Masson-Delmotte, V., Zhai, P., Pirani, A., Connors, S.L., Péan, C., Berger, S., Caud, N., Chen, Y., Goldfarb, L., Gomis, M.I., et al., Eds.; Cambridge University Press: Cambridge, UK; New York, NY, USA, 2021; pp. 1513–1766. [\[CrossRef\]](#)

15. Stefanidis, S.; Alexandridis, V.; Theodoridou, T. Flood Exposure of Residential Areas and Infrastructure in Greece. *Hydrology* **2022**, *9*, 145. [CrossRef]
16. Qiang, Y. Flood exposure of critical infrastructures in the United States. *Int. J. Disaster Risk Reduct.* **2019**, *39*, 101240. [CrossRef]
17. Fujiki, K.; Finance, O. Exposition et Vulnérabilité Sociale des Villes Françaises au Risque Inondation: Une Analyse Spatiotemporelle à Fine Échelle (1999–2017). *Cybergeo Eur. J. Geogr.* **2022**. Available online: <https://journals.openedition.org/cybergeo/39179> (accessed on 3 March 2022). [CrossRef]
18. Centre for Research on the Epidemiology of Disasters (CRED). CRED Crunch 66-Disasters Year in Review. 2021. Available online: <https://cred.be/sites/default/files/CREDCrunch66N.pdf> (accessed on 10 May 2022).
19. Petrucci, O.; Papagiannaki, K.; Aceto, L.; Boissier, L.; Kotroni, V.; Grimalt, M.; Llasat, M.; Llasat-Botija, M.; Rosselló, J.; Pasqua, A.; et al. MEFF: The database of Mediterranean flood fatalities (1980 to 2015). *J. Flood Risk Manag.* **2018**, *122*, e12461. [CrossRef]
20. Papagiannaki, K.; Petrucci, O.; Diakakis, M.; Kotroni, V.; Aceto, L.; Bianchi, C.; Brázdil, R.; Gelabert, M.G.; Inbar, M.; Kahraman, A.; et al. Développer un ensemble de données à grande échelle sur les décès dus aux inondations pour les territoires de la région euro-méditerranéenne, FFEM-DB. *Sci. Data* **2022**, *9*, 166. [CrossRef] [PubMed]
21. Alexander, L.; Zhang, X.; Peterson, T.C.; Caesar, J.; Gleason, B.; Tank, A.M.G.K.; Haylock, M.; Collins, D.; Trewin, B.; Rahimzadeh, F.; et al. Global observed changes in daily climate extremes of temperature and precipitation. *J. Geophys. Res.* **2006**, *111*, D05109. [CrossRef]
22. Dieppois, B.; Durand, A.; Fournier, M.; Diedhiou, A.; Fontaine, B.; Massei, N.; Nouaceur, Z.; Sebag, D. Low-frequency variability and zonal contrast in Sahel rainfall and Atlantic sea surface temperature teleconnections during the last century. *Theor. Appl. Climatol.* **2014**, *121*, 139–155. [CrossRef]
23. Nouacer, Z.; Murarescu, O. Rainfall Variability and Trend Analysis of Annual Rainfall in North Africa. *Int. J. Atmos. Sci.* **2016**, *2016*, 7230450. [CrossRef]
24. Nouaceur, Z. La reprise des pluies et la recrudescence des inondations en Afrique de l’Ouest sahélienne. *Physio-Géo. Géographie Phys. Environ.* **2020**, *15*, 89–109. [CrossRef]
25. Nouaceur, Z.; Laignel, B.; Turki, I. Changements climatiques au Maghreb: Vers des conditions plus humides et plus chaudes sur le littoral algérien? *PhysioGéo* **2013**, *7*, 307–323. [CrossRef]
26. Fontaine, B.; Roucou, P.; Camara, M.; Vigaud, N.; Konare, A.; Sanda, S.; Diedhiou, A.; Janicot, S. Variabilité pluviométrique, changement climatique et régionalisation en région de mousson africaine. *Météorologie* **2012**, *8*, 41. [CrossRef]
27. Criado-Aldeanueva, F.; Soto-Navarro, F.J. The Mediterranean Oscillation Teleconnection Index: Station-Based versus Principal Component Paradigms. *Adv. Meteorol.* **2013**, *2013*, 738501. [CrossRef]
28. Dougrededoit, A. Le climat du bassin méditerranéen. In *Le Climat, l’eau et les Hommes, Ouvrages en l’honneur de Jean Mounier*; Presses Universitaires de Rennes: Rennes, France, 1997; pp. 251–280.
29. Xoplaki, E. Climate Variability over the Mediterranean. Ph.D. Thesis, Diss. Naturwiss. Bern. Literaturverz, University of Bern, Bern, Switzerland, 2002.
30. Boudevillain, B.; Argence, S.; Claud, C.; Ducrocq, V.; Joly, B.; Joly, A.; Lambert, D.; Nuissier, O.; Plu, M.; Ricard, D.; et al. Cyclogenèses et précipitations intenses en région méditerranéenne: Origines et caractéristiques Projet? *Météorologie* **2009**, *8*, 18–28. [CrossRef]
31. Joly, D.; Brossard, T.; Cardot, H.; Cavailles, J.; Hilal, M.; Wavresky, P. Les types de climats en France, une construction spatiale. *Cybergeo Eur. J. Geogr.* **2010**. [CrossRef]
32. Lelièvre, F.; Sala, S.; Ruget, F.; Volaire, F. *Evolution Climatique du Sud de la France 1950–2009, Projet CLIMFOUREL PSDR-3, Régions L-R, M-P, R-A. Série Les Focus PSDR3*; 2011. Available online: <https://studylibfr.com/doc/8236342/evolution-du-climat-du-sud-de-la-france-1950-2009> (accessed on 15 March 2022).
33. Quezel, P. La région méditerranéenne française et ses essences forestières. Signification écologique dans le contexte circum-méditerranéen, forêts méditerranéenne. *Méditerranéenne* **1979**, *1*, 7–18.
34. Rossi, A. Analyse spatio-temporelle de la variabilité hydrologique du bassin versant du Mississippi: Rôles des fluctuations climatiques et déduction de l’impact des modifications du milieu physique. In *Thèse de Géologie-Hydrologie*; Université de Rouen: Rouen, France, 2010; p. 329.
35. Zamrane, Z. Recherche d’indices de variabilité climatique dans des séries hydroclimatiques au Maroc: Identification. positionnement temporel. tendances et liens avec les fluctuations climatiques: Cas des grands bassins de la Moulouya. du Sebou et du Tensift. In *Sciences de la Terre*; Université Montpellier: Montpellier, France, 2016; p. 197.
36. Zamrane, Z.; Mahé, G.; Laftouhi, N.-E. Wavelet Analysis of Rainfall and Runoff Multidecadal Time Series on Large River Basins in Western North Africa. *Water* **2021**, *13*, 3243. [CrossRef]
37. Labat, D. Recent Advances in Wavelet Analyses: Part 1. A Review of Concepts. *J. Hydrol.* **2005**, *314*, 275–288. [CrossRef]
38. Maraun, D. What Can We Learn from Climate Data? Methods for Fluctuation. Time/Scale and Phase Analysis. Ph.D. Thesis, Universität Potsdam, Potsdam, Germany, 2006.
39. Maraun, D.; Kurths, J. Cross wavelet analysis: Significance testing and pitfalls. *Nonlinear Process. Geophys.* **2004**, *11*, 505–514. [CrossRef]
40. Torrence, C.; Compo, G.P. A practical guide to wavelet analysis. *Bull. Am. Meteorol. Soc.* **1998**, *79*, 61–78. [CrossRef]
41. Grossmann, A.; Morlet, J. Decomposition of Hardy Functions into Square Integrable Wavelets of Constant Shape. *SIAM J. Math. Anal.* **1984**, *15*, 723–736. [CrossRef]

42. Jacob, D.; Petersen, J.; Eggert, B.; Alias, A.; Christensen, O.B.; Bouwer, L.M.; Braun, A.; Colette, A.; Déqué, M.; Georgievski, G. EURO-CORDEX: New high-resolution climate change projections for European impact research. *Reg. Environ. Change* **2014**, *14*, 563–578. [[CrossRef](#)]
43. Thévenot, O.; Bouin, M.-N.; Ducrocq, V.; Brossier, C.L.; Nuissier, O.; Pianezze, J.; Duffourg, F. Influence of the sea state on Mediterranean heavy precipitation: A case-study from HyMeX SOP1. *Q. J. R. Meteorol. Soc.* **2016**, *142*, 377–389. [[CrossRef](#)]
44. Rowell David, P. The Impact of Mediterranean SSTs on the Sahelian Rainfall Season. *J. Clim.* **2003**, *16*, 849–862. [[CrossRef](#)]
45. Peyrille, P.; Lafore, J.P. An idealized two-dimensional framework to study the West African monsoon. Part II: Large-scale advection and the diurnal cycle. *J. Atmos. Sci.* **2007**, *64*, 2783–2803. [[CrossRef](#)]
46. Somot, S.; Sevault, F.; Déqué, M.; Crépon, M. 21st century climate change scenario for the Mediterranean using a coupled atmosphere–ocean regional climate model. *Glob. Planet. Chang.* **2008**, *63*, 112–126. [[CrossRef](#)]
47. Kharin, V.; Zwiers, F.; Zhang, X.; Wehner, M. Changes in temperature and precipitation extremes in the CMIP5 ensemble. *Clim. Change* **2013**, *119*, 345–357. [[CrossRef](#)]
48. O’Gorman, P.A. Precipitation extremes under climate change. *Curr. Clim. Change Rep.* **2015**, *1*, 49–59. [[CrossRef](#)]
49. Madakumbura, G.D.; Thackeray, C.W.; Norris, J.; Goldenson, N.; Hall, A. Anthropogenic influence on extreme precipitation over global land areas seen in multiple observational datasets. *Nat. Commun.* **2021**, *12*, 3944. [[CrossRef](#)] [[PubMed](#)]
50. Folland, C.; Palmer, T.; Parker, D. Sahel rainfall and worldwide sea temperatures, 1901–1985. *Nature* **1986**, *320*, 602–607. [[CrossRef](#)]
51. Giannini, A.; Saravanan, R.; Chang, P. Oceanic forcing of Sahel rainfall on interannual to interdecadal time scales. *Science* **2003**, *302*, 1027–1030. [[CrossRef](#)]
52. Held, I.M.; Delworth, T.L.; Lu, J.; Findell, K.L.; Knutson, T.R. Simulation of Sahel drought in the 20th and 21st centuries. *PNAS* **2005**, *102*, 17891–17896. [[CrossRef](#)]
53. Biasutti, M.; Gianini, A. Robust Sahel drying in response to late 20th century forcings. *Geophys. Res. Lett.* **2006**, *33*. [[CrossRef](#)]
54. Caminade, C.; Terray, L. Twentieth Century Sahel Rainfall Variability as Simulated by the ARPEGE AGCM, and Future Changes. *Clim. Dyn.* **2010**, *35*, 75–94. [[CrossRef](#)]
55. Biasutti, M. Forced Sahel rainfall trends in the CMIP5 archive. *JGR Atmos.* **2013**, *111*, 1613–1623. [[CrossRef](#)]
56. Zhang, R.; Delworth Thomas, L. Impact of Atlantic multidecadal oscillations on India/Sahel rainfall and Atlantic hurricanes. *Geophys. Res. Lett.* **2006**, *33*, L17712. [[CrossRef](#)]
57. Martin-Vide, J.; Lopeiz-Bustins, J.A. The Western Mediterranean Oscillation and Iberian Peninsula Rainfall. *Int. J. Climatol.* **2006**, *26*, 1455–1475. [[CrossRef](#)]
58. Skinner, C. Statistical Disclosure Risk: Separating Potential and Harm. *Int. Stat. Rev.* **2012**, *80*, 349–368. [[CrossRef](#)]
59. Conte, M.; Giuffrida, A.; Tedesco, S. The Mediterranean Oscillation, impact on precipitation and hydrology in Italy. In *Conference on Climate Water*; Publications of the Academy of Finland: Helsinki, Finland, 1989; pp. 121–137.
60. Törnros, T. On the relationship between the Mediterranean Oscillation and winter precipitation in the Southern Levant. *Atmos. Sci. Lett.* **2013**, *14*, 287–293. [[CrossRef](#)]
61. Sakalli, A. Sea surface temperature change in the mediterranean sea under climate change: A linear model for simulation of the sea surface temperature up to 2100. *Appl. Ecol. Environ. Res.* **2017**, *15*, 707–716. [[CrossRef](#)]
62. Mizuta, R.; Arakawa, O.; Ose, T.; Kusunoki, S.; Endo, H.; Kitoh, A. Classification of CMIP5 future climate responses by the tropical sea surface temperature changes. *SOLA* **2014**, *10*, 167–171. [[CrossRef](#)]
63. Pastor, F.; Valiente, J.A.; Estrela, M.J. Sea surface temperature and torrential rains in the Valencia region: Modelling the role of recharge areas. *Nat. Hazards Earth Syst. Sci.* **2015**, *15*, 1677–1693. [[CrossRef](#)]
64. Pastor, F.; Valiente, J.A.; Palau, J.L. Sea Surface Temperature in the Mediterranean: Trends and Spatial Patterns (1982–2016). *Pure Appl. Geophys.* **2018**, *175*, 4017. [[CrossRef](#)]